

Nonequilibrium nuclear-electron spin dynamics in semiconductor quantum dots

D. H. Feng, I. A. Akimov, and F. Henneberger

Institut für Physik, Humboldt Universität zu Berlin, Newtonstr.15, 12489 Berlin, Germany

(dated: March 23, 2024)

We study the spin dynamics in charged quantum dots in the situation where the resident electron is coupled to only about 200 nuclear spins and where the electron spin splitting induced by the Overhauser field does not exceed markedly the spectral broadening. The formation of a dynamical nuclear polarization as well as its subsequent decay by the dipole-dipole interaction is directly resolved in time. Because not limited by intrinsic nonlinearities, almost complete nuclear polarization is achieved, even at elevated temperatures. The data suggest a nonequilibrium mode of nuclear polarization, distinctly different from the spin temperature concept exploited on bulk semiconductors.

PACS numbers: 72.25.Fe, 78.67.Hc, 78.55.Et, 72.25.Rb

The hyperfine interaction of the electron with the nuclear spins in semiconductor quantum dots has become recently a focus of both theoretical and experimental research. In the absence of external magnetic fields, it governs the timescale on which the electron spin can be stored and manipulated. The dynamical scenario depends sensitively on the state of the nuclear system as well as on the type of average performed in the experiment [1, 2, 3]. On the other hand, continuous pumping of the electron spin can generate through hyperfine-mediated spin flips a dynamical nuclear polarization (DNP). It is important to distinguish between nonequilibrium and equilibrium DNP [4]. The nonequilibrium DNP is destroyed by the nuclear dipole-dipole interaction with a time constant (τ_{dd}) of about 10^{-4} s. In bulk semiconductors, because of the huge number of nuclear spins seen by the electron, the formation time (τ_F) of the DNP is much longer than the dipole-dipole decay, ruling out a significant nonequilibrium mode. However, spin temperature cooling in an external magnetic field can produce an equilibrium DNP. The field Zeeman-splits the nuclear states sufficiently up and selectively pumping one of the populations via the flip-flop process creates a nuclear spin temperature different to that of the lattice [5]. The decay of the equilibrium DNP requires dissipation of the Zeeman energy by spin-lattice interaction which takes place on timescales of a second and beyond. It has been argued that an external field is not required for quantum dots, as the hyperfine Knight field is strong enough to ensure spin cooling conditions [6, 7]. For InAs/GaAs structures, the presence of the DNP is directly displayed by a zero-field splitting of the dot emission [6]. The Overhauser field can reach here the 1-Tesla range and gives rise to strong nonlinearities in the electron spin occupation [8]. The DNP formation time estimated from indirect measurements is $\tau_F \sim 1$ s [6, 8]. In this Letter, we investigate Stran'ski-Krastanov CdSe/ZnSe quantum dots which have a 2-3 orders of magnitude smaller volume size. We directly demonstrate that these quantum dots realize the unique situation $\tau_F < \tau_{dd}$ allowing for – unlike the vast amount

of previous work on semiconductors – the formation of a strong nonequilibrium DNP.

The quantum dot structures are grown by molecular beam epitaxy. Making use of the native n-type of these materials, dots charged with a resident electron are formed under appropriate stoichiometry conditions. Transmission electron microscopy provides a dot height of below 2 nm and a lateral extension below 10 nm [9]. The optical measurements are performed in a confocal arrangement with the propagation direction of incident and emitted light parallel to the [001] growth axis. The sample is placed in a He-flow cryostat capable of variable temperature and magnetic fields up to $B = 5$ T. Quasi-resonant excitation of the trion feature (2 electrons, 1 hole) by circularly polarized light constitutes a very efficient spin pumping mechanism for the resident electron [7]. In turn, the secondary emission from the trion directly monitors the electron spin polarization achieved. Trains of rectangular light pulses with a duration t_{on} spaced by a dark time t_{dark} are generated from a cw laser by means of an acousto-optical modulator (Fig. 1a). Use of a properly triggered Pockels cell allows for the generation of sequences with alternating $\sigma^+ =$ polarization or with σ^+ polarization only. A difficulty of the measurements is an increasing number of dark counts when t_{dark} exceeds considerably t_{on} . The data presented below are selectively verified on a single-dot level, systematic studies at reasonable integration times are made on ensembles with a much better signal-to-noise ratio. The external magnetic field is always directed along the electron spin.

Fig. 1 summarizes the main features of the experiment. Because of the anti-parallel spins of the two electrons, the total trion spin is defined by the hole and is thus $S=2$. This provides the circular polarization selection rules $j=1 \rightarrow 2$ and $j=3 \rightarrow 2$ of the electron-trion transition. In order to suppress stray light, the trion is quasi-resonantly excited with 1-LO phonon energy in excess through a polaron-like state. This state has the same spin structure as the trion ground-state and obeys hence the same selection rules. Excitation, say with σ^+ pho-

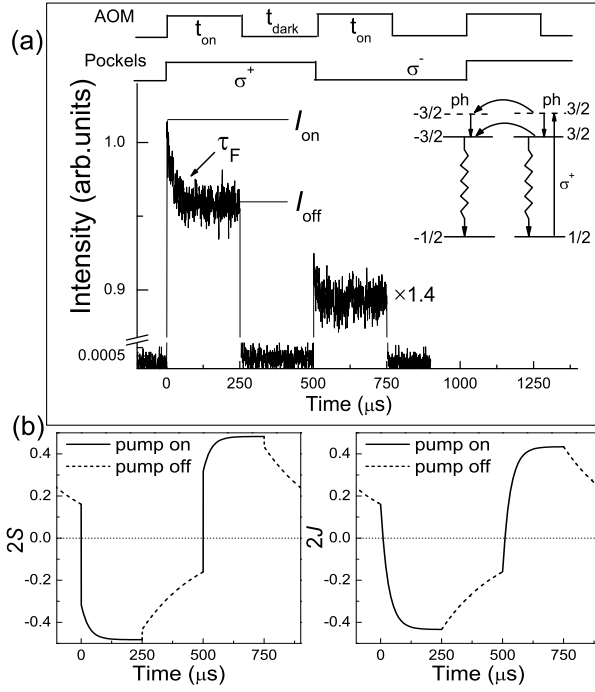


FIG. 1: Electron-nuclear dynamics as revealed by quasi-resonant excitation of the trion feature. (a) Optical excitation trains in alternating polarization mode (top) as well as PL transients (main panel) recorded at $T = 60$ K and $B = 0$. Excitation intensity is 2 kW/cm^2 . Excitation and detection (1-LO-phonon below) is on the low-energy wing of the ensemble PL band centered at about 2.43 eV . Detection is in $+$ polarization. The different signal levels in $+$ and pumping reflect the degree of hole spin relaxation in the trion [14]. detection just reverses these levels. For more details about the experimental setup see [7]. Right inset: Optical transition scheme underlying the electron spin pumping for $+$ photons. A flip of the $3/2$ hole spin in the trion directs the excitation to the other arm so that a spin-down electron is left behind after recombination (ph : trion-LO-phonon state). (b) Calculated electron and nuclear spin transients from equations (1) with parameters $N = 200$; $\tau_e = 50 \text{ ns}$, $\hbar A = 6 \text{ eV}$, $\tau_c = 1.2 \text{ ns}$, $\tau_{d-d} = 250 \text{ } \mu s$.

tons, removes thus selectively a spin-up electron. The polaron-trion state relaxes rapidly to the trion ground-state which subsequently radiatively decays within about 500 ps . When the hole spin-flips, a spin-down electron is left behind. More precisely, denoting by $\rho_{\uparrow\uparrow}$ and $\rho_{\downarrow\downarrow}$ the diagonal elements of the electron spin density matrix, $\rho_{\uparrow\uparrow}$ is increased at the expense of $\rho_{\downarrow\downarrow}$ or, in other words, an average spin $S = (\rho_{\uparrow\uparrow} - \rho_{\downarrow\downarrow})/2 < 0$ just opposite to the excitation photon momentum is formed. The associated depletion of the spin-up initial state in absorption decreases the trion excitation rate $\rho_{\downarrow\downarrow} = 1/2 + S$ and, in the same way, the photoluminescence (PL) signal emitted by the dot (independent on the photon polarization detected). The experimental PL transients in Fig. 1 reveal therefore directly an increasing electron

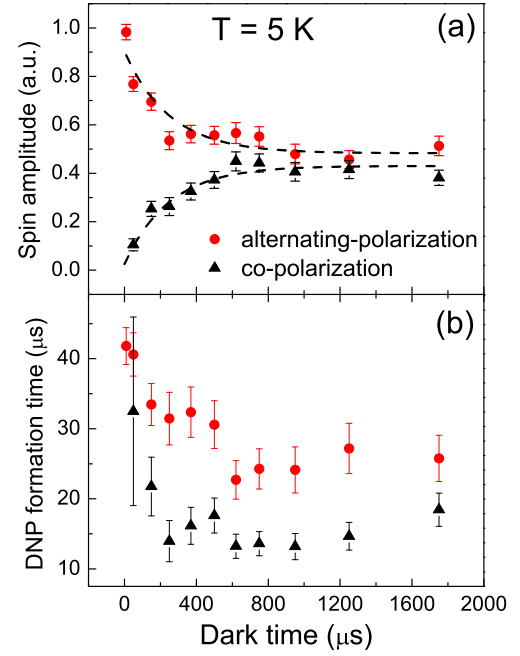


FIG. 2: Spin amplitude (a) and DNP formation time (b) as functions of the dark time in both polarization modes ($B = 0$). The dashed curves are single-exponential fits with a time constant of $250 \text{ } \mu s$.

spin alignment during pumping. The spin amplitude S generated is proportional to $(I_{on} - I_{off})/I_0$ and the characteristic time for its formation (τ_F) is taken at the $1/e$ point of the transients. Fig. 2 depicts both quantities as a function of the dark time. During the dark period, electron as well as nuclear spin decay down to a certain level. Restarting pumping enables us to study the spin dynamics at different initial polarizations. Complete loss of the spin memory from the previous pulse has happened when the amplitudes in alternating and co-polarization become equal. As evident from Fig. 2, this time is considerably longer than the few $10 \text{ } \mu s$ needed for the build-up of the amplitude.

The electron-nuclear spin dynamics revealed by the above measurements is well described by the equations

$$\begin{aligned} \frac{dS}{dt} &= \frac{1}{2}P - \frac{S}{\tau_e} + N \frac{J}{\hbar f} \frac{S}{\tau_{hf}}; \\ \frac{dJ}{dt} &= \frac{S}{\tau_{hf}} - \frac{J}{\tau_{d-d}}; \end{aligned} \quad (1)$$

considering neither inhomogeneity of the hyperfine coupling nor collective effects in the nuclear system [10]. The

sign at the spin pumping rate P stands for excitation and $N = aN_L$ with the effective number N_L of lattice atoms surrounding the electron and the isotope abundance a . The isospin of Cd and Se is $1/2$ so that the nuclear average spin J per isotope is analogously defined as for the electron. τ_e summarizes the lifetime of the electron in the dot as well as all spin relaxation processes

aside from the hyperfine interaction. If only the hyperfine contribution (characterized by a single time τ_{hf}) is accounted for, these equations ensure total spin conservation $S + N_J = 0$. The linear system is easily solved analytically yielding two time constants by which the steady-state values $S_{st} = P_e(\tau_{hf} + \tau_{dd})/2(\tau_{hf} + \tau_{dd} + N_e)$ and $J_{st} = S_{st} \tau_{dd}/(\tau_{hf} + \tau_{dd})$ are approached. The sole electron spin pumping scenario is studied by eliminating the hyperfine coupling by an external magnetic field of $B = 100$ mT [7]. The electron lifetime is power-dependent $1/\tau_e = P + P_0$, both intrinsically due to the excitation process itself as well as due to dot recharging by carriers generated in the environment as a side effect ($\tau_e \propto 1/P$). Specifically, this generates a spin polarization $2S = P_e$ of close to 0.5 depending only weakly on the pumping rate. At the power of the present measurements $P_e = 50$ ns. During pumping, it holds thus $\tau_e \approx \tau_{dd}$ which provides in lowest order

$$\begin{aligned} S(t) &= S_0 e^{-t/\tau_1} - J_0 K (e^{-t/\tau_1} - e^{-t/\tau_2}); \\ J(t) &= J_0 e^{-t/\tau_2}; \end{aligned}$$

for the deviations from steady state. The times τ_1 and τ_2 are very much different for $N_e \gg 1$. The short component $\tau_1 = \tau_e \tau_{hf}/(\tau_{hf} + N_e)$, not resolved on the timescale of Fig. 1, describes the direct response of the electron on spin pumping, whereas $\tau_2 = (\tau_{hf} + N_e)/(1 + \tau_{hf}/\tau_{dd} + N_e/\tau_{dd})$ represents the DNP formation time τ_F (shown in Fig. 2b) and $K = N_e/(\tau_{hf} + N_e)$ measures the degree by which the presence of the DNP increases the electron spin polarization. During the dark period ($P; S_{st}; J_{st} = 0$), τ_e is orders of magnitude longer so that now the single-spin flip defines the shortest timescale ($\tau_{hf} = N_e \tau_{dd}$; τ_{dd} ; τ_e) providing $\tau_1 = \tau_{hf} = N_e \tau_{dd}$, $\tau_2 = \tau_{dd}$, and $K = 1$. The short τ_1 enforces $S \approx J$, while both polarizations decay slowly by τ_{dd} . Application of periodic boundary conditions results in spin amplitudes $S = S_1 [1 - \exp(-\tau_{dark}/\tau_{dd})]$ for alternating and co-polarization mode, respectively, where $S_1 = K J_{st} (\tau_{on}/\tau_F)$. The experimental data in Fig. 2a follow closely this prediction yielding $\tau_{dd} = 250$ s. The formation time of the DNP is hence about one order of magnitude shorter than its decay by the dipole-dipole interaction.

The linewidth broadening of the electron spin levels is determined by the lifetime of the off-diagonal density matrix elements $\rho_{\alpha\beta}$. Denoting this time by τ_c and assuming $(A/N_L) \tau_c \gg 1$ leads to the standard expression $1/\tau_{hf} = 1/\tau_{Le} = (A/N_L)^2 \tau_c = (1 + \beta_B^2/\beta_c^2)$ [11] where β_B represents the electron Zeeman splitting [17]. For no external field, the nuclear Overhauser field associated with the DNP provides $\beta_B = aA J$. This term introduces nonlinearities in the dynamics which inhibit the formation of the DNP by increasing the formation time [8]. A distinct feature of the experimental findings is a continuous increase of S during spin pumping, also in alternating

polarization mode (Fig. 1a). Here, the nuclear spin reverses sign so that $1/\tau_{hf}$ changes from slow to fast to slow and the electron spin would pass through a minimum if aA_c was markedly larger than 1. A weak Overhauser feedback is also signified by the dark-time dependence of the DNP formation time (Fig. 2b). Indeed, τ_F is longer for smaller τ_{dark} because of a stronger initial DNP, but the overall change is only about 30%. Solving equations (1) numerically with the Overhauser field included yields $aA_c = 1.4$. This value is consistent with the asymmetries of the spin transients observed in a weak external magnetic field [7]. The present quantum dots define thus a regime where the DNP-induced spin splitting does not exceed markedly the broadening of the Zeeman levels.

The fast DNP formation time of a few 10 s is in accordance with the hyperfine parameters of CdSe quantum dots. The electron wavefunction ψ_e obtained by calculating the energy position of the ensemble PL provides an average number $N_L = 8 = (v_0 \int |\psi_e|^4(r) dV) / 1600$ (v_0 : volume of unit cell) [12]. Accounting for only the major contribution from the $^{111};^{113}\text{Cd}$ isotopes ($a = 0.125$), it follows that merely $N = 200$ atoms carry a nuclear moment. For $\chi_I^{\text{Cd}} = -0.6$, we estimate $\sim A = 6$ eV [13]. The disappearance of the DNP-related spin amplitude in an external field of some 10 mT ($\beta_B = 9$ ns $^{-1}$ $B = 100$ mT) provides $\tau_c \approx 1$ ns [7]. Combining these data, it follows $aA_c \approx 1$ and $\tau_{hf} \approx 25$ s. Hyperfine flip-ops and electron lifetime ($N_e \approx 10$ s) contribute thus about equally to the DNP formation time ($K \approx 0.5$). Spin transients computed for the above parameters predict virtually the same nuclear and electron spin polarizations (Fig. 1b). Full closing of the hyperfine flip-ops rates is experimentally corroborated by single-dot measurements. The zero-field transients approach the same final value as the fast transients at $B = 100$ mT of $2S \approx 0.5$.

The DNP formation time shortens monotonically with temperature, while the spin amplitude initially slightly increases reaching a maximum at about 50 K before it starts to decline (Fig. 3). A shorter τ_F at higher temperature is expected from the shortening of the electron lifetime. The temperature increase of the amplitude is consistent with the behavior of the pumping rate. At given optical power, P increases first as the hole spin flip in the trion state becomes faster [14]. Subsequently, the shortening of the electron lifetime takes over. Single-dot measurements where contribution of nontrionic origin can be excluded confirm these tendencies.

After elaboration of the formation dynamics we deal finally with the decay of the DNP by the dipole-dipole interaction. The 250 s decay time is in accord with the interaction energy of 10^{-5} eV of neighboring nuclei. Standard spin cooling is described by a depolarization time $\tau_B^2 = \tau_L^2$ where τ_L is the effective local dipole field [15]. A substantial Knight field B_K/S added to B [6, 7] would show up by an asymmetry of the decay transients with respect to the directions of electron spin

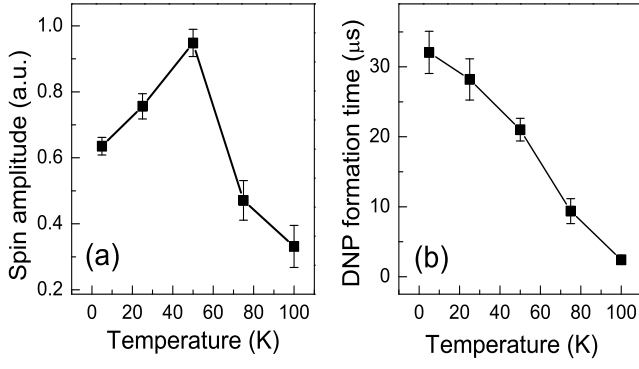


FIG. 3: Temperature dependence of (a) spin amplitude and (b) formation time for $t_{\text{dark}} = 0$ taken in alternating polarization mode ($B = 0$).

and external field. No such asymmetry is found beyond the experimental resolution. The magnetic-field dependence of the dipole-dipole time is depicted in Fig. 4a. It increases about one order of magnitude for modest field strength ($B = 5$ mT), clearly demonstrating the opening of a nuclear spin splitting suppressing dipole-dipole-mediated transitions between different nuclei. The zero-field time decreases only smoothly with temperature (Fig. 4b) so that the relation $T_F < t_{\text{d-d}}$ is maintained up to 100 K. Measurements on an extended time scale (Fig. 4c) uncover in addition to the 100 μ s component a second, clearly smaller part which persists up to the millisecond range. This part becomes increasingly visible at higher temperature and makes up a 0.2 portion of the total amplitude at 60 K. The origin of the long persisting DNP needs further investigations. It might be due to the Se isotopes with lower abundance or spin diffusion between different dots.

In summary, we have demonstrated the formation of a strong nonequilibrium DNP at zero external magnetic field. A number of only a few 100 nuclei and a weak Overhauser field allow for the creation of the DNP in a time much shorter than in the standard spin cooling protocol. The Knight field does not play an essential role. We have found an intrinsic zero-field dipole-dipole decay time of about 250 μ s. The nuclear polarization is complete in the sense that it reaches the level of the available electron spin. Minimizing dot recharging under injection by structure improvement will permit to approach the ultimate limit $2S/2J \approx 1$. Signatures of a DNP formation are seen up to about 100 K. At those temperatures, the optical spin pumping and read-out via the trion features break down. Whether or not a DNP can be established at still higher temperatures can not be decided by the present experiments. The measurements suggest a very short electron spin correlation time $\tau_c \approx 1$ ns under optical pumping. Spin exchange processes with carriers excited in the dot environment [16] seem to play an essential role in Stranski-Krastanov structures.

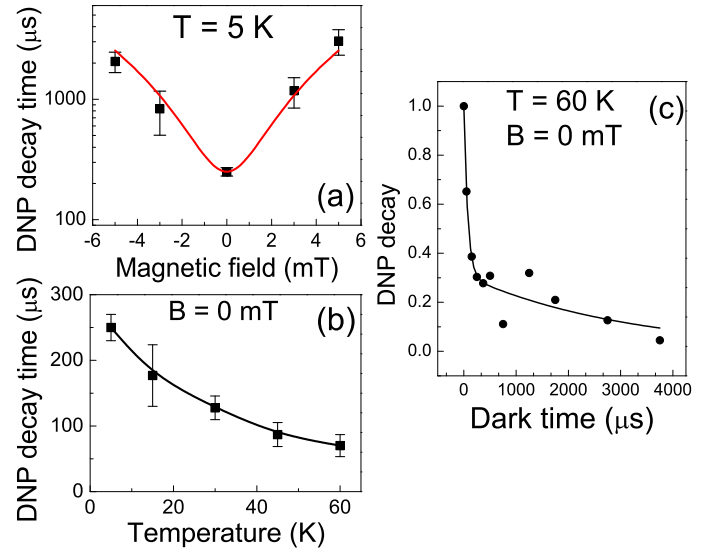


FIG. 4: Dynamics of the DNP decay. (a) Magnetic field dependence of the decay time obtained from single-exponential fits to the experimental $(S_{\text{al}} - S_{\text{co}}) = (S_{\text{al}} + S_{\text{co}})$ for lower noise. The line represents $t_{\text{d-d}}(B) = 250 \text{ s} + 91 \text{ s/mT } B^2$. (b) Temperature dependence. (c) Decay transient at elevated temperature on a longer time scale.

This work was supported by the Deutsche Forschungsgemeinschaft with in Project No. He 1939/18-1.

-
- [1] I. A. Merkulov, A. L. Efros, and M. Rosen, Phys. Rev. B 65, 205309 (2002).
 - [2] P. F. Braun et al., Phys. Rev. Lett. 94, 116601 (2005).
 - [3] A. V. Khaetskii, D. Loss and L. Glazman, Phys. Rev. Lett. 88, 186802 (2002); Phys. Rev. B 67, 195329 (2003); W. A. Coish and D. Loss, *ibid.* 70, 195340 (2004).
 - [4] V. G. Fleisher and I. A. Merkulov in Optical Orientation, ed. F. Meier and B. P. Zakharchenya, (North Holland, Amsterdam, 1984) p. 173; M. I. Dyakonov and V. I. Perel, *ibid.*, p. 11.
 - [5] A. Abragam and W. G. Proctor, Phys. Rev. 109, 1441 (1953).
 - [6] C. W. Lai et al., Phys. Rev. Lett. 96, 167403 (2006).
 - [7] I. A. Akimov, D. H. Feng, and F. Henneberger, Phys. Rev. Lett. 97, 056602 (2006).
 - [8] P. F. Braun et al., Phys. Rev. B 74, 245306 (2006); P. Maletinsky et al., *ibid.* 75, 035409 (2007); A. I. Tartakovskii et al., Phys. Rev. Lett. 98, 026806 (2007).
 - [9] D. Litvinov et al., Appl. Phys. Lett. 81, 640 (2002).
 - [10] Such effects are treated by H. Christ, J. I. Cirac, and G. Giedke, Phys. Rev. B 75, 155324 (2007).
 - [11] M. I. Dyakonov and V. I. Perel, Sov. Phys. JETP 38, 177 (1974).
 - [12] P. R. Kratzert et al., Appl. Phys. Lett. 79, 2814 (2001); A. Hundt, J. Puls, and F. Henneberger, Phys. Rev. B 69, 121309(R) (2004).
 - [13] We use the Bloch factor $j(\tau_c \Delta)^2 = 2200$ from CdTe: A. Nakamura et al., Solid State Commun. 30, 411 (1979).

- [14] T. Flissikowski et al., Phys. Rev. B 68, 161309(R) (2003).
- [15] D. Gamm on et al., Phys. Rev. Lett. 86, 5176 (2001).
- [16] D. Paget, Phys. Rev. B 25, 4444 (1989); see also: R. I. Dzhioev et al., Phys. Rev. Lett. 88, 256801 (2002).
- [17] The splitting of the nuclear levels can be neglected.